

Drastic change of the Casimir force at the metal-insulator transitionE. G. Galkina,^{1,2} B. A. Ivanov,^{1,3,4,*} Sergey Savel'ev,^{1,5} V. A. Yampol'skii,^{1,6} and Franco Nori^{1,7}¹*Advanced Science Institute, The Institute of Physical and Chemical Research (RIKEN), Wako-shi, Saitama 351-0198, Japan*²*Institute of Physics, 03028 Kiev, Ukraine*³*Institute of Magnetism, 03142 Kiev, Ukraine*⁴*National T. Shevchenko University of Kiev, 03127 Kiev, Ukraine*⁵*Department of Physics, Loughborough University, Loughborough LE11 3TU, United Kingdom*⁶*A. Ya. Usikov Institute for Radiophysics and Electronics, 61085 Kharkov, Ukraine*⁷*Department of Physics, Center for Theoretical Physics, Applied Physics Program, The University of Michigan, Ann Arbor, Michigan 48109-1040, USA*

(Received 1 August 2008; revised manuscript received 13 August 2009; published 22 September 2009)

The dependence of the Casimir force on material properties is important for both future applications and to gain further insight on its fundamental aspects. Here we apply the general Lifshitz theory of the Casimir force to low-conducting compounds, or poor metals. For distances in the micrometer range, the Casimir force for a large variety of such materials is described by universal equations containing a few parameters: the effective plasma frequency ω_p , dissipation rate γ of the free carriers, and electric permittivity ϵ_∞ for $\omega \geq \omega_p$ (in the infrared range). This theory of the Casimir force for poor metals can also describe inhomogeneous composite materials containing small regions with different conductivity. The Casimir force for systems involving samples made with compounds that have a metal-insulator transition shows a drastic change of the Casimir force within the transition region, where the metallic and dielectric phases coexist. Indeed, the Casimir force can increase by a factor of 2 near this transition.

DOI: [10.1103/PhysRevB.80.125119](https://doi.org/10.1103/PhysRevB.80.125119)

PACS number(s): 78.20.Ci, 11.10.Wx

I. INTRODUCTION AND MOTIVATION

The Casimir force¹ has demonstrated the reality of zero-point field fluctuations, which played a significant role in the development of quantum-field theory (see, e.g., the monographs^{2,3} and review papers⁴⁻⁷). The Casimir effect attracts considerable attention because of its numerous applications in quantum-field theory, atomic physics, condensed-matter physics, gravitation, and cosmology.²⁻¹⁰ The experimental observation of the Casimir force is of fundamental importance. Despite the fact that the magnitude of the Casimir force is quite small, its presence is established by a number of experiments, usually done for metallic samples; see, e.g., Refs. 10–15. Furthermore, this force is relevant for various nanomechanical devices, where the space separation of nearby plates is very small.^{3,6,16}

A. Casimir force for good metals and dielectrics

The Casimir force between two macroscopic samples is caused by a spatial redistribution of the fluctuations of the electromagnetic field compared to that of free space because of the presence of the samples. For the simplest case of two parallel *perfectly conducting* thick metallic plates placed in vacuum and separated by a distance l , the Casimir force per unit area of the sample at zero temperature can be written as

$$F_C = \frac{\pi^2}{240} \frac{c\hbar}{l^4}, \quad (1)$$

where c is the speed of light and \hbar is the Planck's constant. For *dielectric* bodies with frequency-dependent dielectric permittivities, the value of this force has been found by Lifshitz.¹⁷ If the permittivity ϵ is frequency independent, for

two equivalent dielectric bodies or for a dielectric sample and an ideal metal, this force can be written as

$$F_L = \frac{\pi^2}{240} \frac{c\hbar}{l^4} \cdot \left(\frac{\epsilon - 1}{\epsilon + 1} \right)^\nu \varphi_\nu(\epsilon), \quad (2)$$

where $\nu=2$ for two equivalent dielectric bodies and $\nu=1$ for the interaction of a dielectric sample and a metal. The function $\varphi_\nu(\epsilon) \rightarrow 1$ when $\epsilon \gg 1$ and $\varphi_\nu(\epsilon)$ decreases when $\epsilon \rightarrow 1$; in particular, $\varphi_1(\epsilon \rightarrow 1) = 0.46$ and $\varphi_2(\epsilon \rightarrow 1) = 0.35$. Strictly speaking, equations of type (1) and (2) are valid when $l < \hbar c/kT$, where only the zero-point fluctuations of the electromagnetic field are important (see Refs. 5, 18, and 19 for details). At room temperature, this inequality is valid for distances less than a few micrometers. Below we will only consider this range.

B. Material aspects of the Casimir force

To study the Casimir force, different materials can be used. Indeed, it is important to understand *how* this force is affected by the choice of *different materials*. For example, recent studies, using silicon with different degrees of doping or materials for sensors, such as vanadium oxide,²⁰ have shown numerous specific features which are absent in the good metals traditionally used to study the Casimir force.

The investigation of material-dependent features of the Casimir force is important not only for future applications but also for fundamental physics. To discuss the material-dependent aspects of the Casimir force, let us note the following. The well-known results present in the expressions (1) and (2) were obtained for constant values of the electrical permittivity ϵ , independent of both frequency and wave vector. For metals, this means $\epsilon = \infty$ for any frequency. Taking

into account the temporal and, especially, spatial dispersions is a very complicated problem. Detailed investigations, taking into account the dispersion of the media, have shown^{18,19} that the usual formula of the type $F_C \propto 1/l^4$ is valid for distances $l > l_0$, where $l_0 = c/\omega_0$, and ω_0 is the highest characteristic frequency of the medium. Recently, the spatial dispersion of the permittivity has been shown to be important for describing the effects of thermal fluctuations in the Casimir force, see Refs. 21–23. We do not discuss such effects in this paper and, therefore, do not take into account the spatial dispersion.

For an arbitrary frequency dependence of the permittivity, the Casimir force F can be written^{5,17–19} as

$$F = \frac{\hbar}{2\pi^2 c^3} \cdot \int_0^\infty \zeta^3 d\zeta \cdot \Phi[\varepsilon(i\zeta)], \quad (3)$$

where $\varepsilon = \varepsilon(i\zeta)$ is the complex permittivity of the media, the summation over the Matsubara frequencies is replaced by integration over ζ (this is adequate¹⁸ when $l < \hbar c/kT$), $\Phi[\varepsilon(i\zeta)]$ is a functional of the function $\varepsilon(i\zeta)$,

$$\Phi[\varepsilon(i\zeta)] = \int_1^\infty p^2 dp \left(\frac{1}{A_1^\nu e^x - 1} + \frac{1}{A_2^\nu e^x - 1} \right),$$

$$A_1 = \frac{s+p}{s-p}, \quad A_2 = \frac{p\varepsilon+s}{p\varepsilon-s}, \quad s = \sqrt{\varepsilon + p^2 - 1}, \quad (4)$$

where $x = 2p\zeta l/c$. Two terms in Eq. (4) describe the contributions of the modes with two different polarizations of the electric field parallel to the surface and parallel to the incidence plane (which includes the normal to the surface and the wave vector of the photon), respectively. The exponents $\nu=2$ and $\nu=1$ correspond to the same cases as for Eq. (2), namely, the interaction between two equivalent dispersive media ($\nu=2$), and dispersive medium, interacting with an ideal metal ($\nu=1$). The general properties of the function $\varepsilon(i\zeta)$ are the following: $\varepsilon(i\zeta)$ is a monotonic function of ζ and $\varepsilon(\zeta) \rightarrow 1$ for the values of ζ higher than all the characteristic frequencies of the medium $\zeta > \omega_0$. For metals, the plasma frequency ω_p is the highest frequency ω_0 . Thus, the standard Casimir result Eq. (1) is valid for large distances $l > l_p = c/\omega_p$ between the plates, see Ref. 18. Note that the parameter l_p can be easily estimated through the wavelength of light λ_p , corresponding to plasma frequency $\lambda_p = 2\pi l_p = 2\pi c/\omega_p$, which is usually reported in experimental articles. For the opposite limit case¹⁸ of smaller distances, $l < l_p$,

$$F(l \rightarrow 0) = \frac{\hbar}{8\pi^2 l^3} \bar{\omega}, \quad \bar{\omega} = \int_0^\infty \left(\frac{\varepsilon - 1}{\varepsilon + 1} \right)^\nu d\zeta, \quad (5)$$

where the real dispersion, e.g., the dependence of the media permittivity on the frequency, is used.

C. Caviats and limitations

It is worth noting here that, as far as we know, only one experiment¹² has been performed using the parallel-plate configuration originally envisioned by Casimir. Most measurements of the Casimir force have studied the interaction

of a spherical probe with a flat substrate using the so-called proximity force theorem²⁴ to relate the force for different geometries of the experiment to the force between two parallel plates. The experimental search for corrections to this approximation has been done recently.²⁵ For the original plane-parallel geometry, the accuracy of the measurements¹² of the Casimir force, done for distances of fractions of micrometers, is not very high, but within 15%. A significant difficulty has been the necessity to keep the samples parallel during the measurements at different distances. Some of these problems, in principle, could be overcome by measuring the Casimir force in a fixed geometry of the experiment (fixed l , for plane-parallel geometry) by varying some parameters of the sample. The physical properties of the media could be significantly changed by varying the temperature of the sample. Some changes in the Casimir energy might have been observed when a sample changes to its superconducting state.²⁶ Varying the carrier density of semiconductors by laser irradiation has also been proposed recently,²⁰ as another way to change the Casimir force.

The Casimir force for standard metals has a weak temperature dependence. For metals, the Drude formula, $\varepsilon = 1 + \omega_p^2/\zeta(\zeta + \gamma)$ is typically used, where ω_p is the metal plasma frequency and γ is the relaxation rate. For typical metals such as copper, aluminum, or gold, the plasma frequency is practically temperature independent and the only way to modify the Casimir force by changing the metal parameters is via the temperature dependence of γ . For such metals, $\gamma \ll \omega_p$, and the corresponding corrections are small. Another problem: for standard metals the value of $\lambda_p = 2\pi c/\omega_p$ lies in the ultraviolet region, $\lambda_p \leq 0.1 \mu\text{m}$. Thus, to observe dispersive effects, the region $l \leq \lambda_p$ should be investigated, which is quite difficult¹⁴ (however, possible²⁷) experimentally. This difficulty could be overcome by using thin metallic films²⁸ or bulk dirty and/or large metal samples,²⁹ but even for these optimal cases the temperature corrections are not higher than a few percent.

D. Casimir force for pure metals and compounds

Numerous compounds are known for which the carrier density and plasma frequency ω_p are abnormally small. The investigation of such conducting systems, which can be called “poor metals,” is of interest from the point of view of both fundamental physics and applications. Examples include highly doped silicon,²⁰ left-handed materials,³⁰ transition-metal oxides showing the metal-insulator transition,³¹ cuprate high-temperature superconductors,³² and manganites where the phenomenon of colossal magnetoresistance is observed.³³ For all of these systems, both the free carrier density and the plasma frequency ω_p are much smaller than for standard good metals. This means, that in contrast to the usual metals, ω_p is not the highest frequency of the material. The Drude behavior is observed up to infrared frequencies but with a relatively large value of $\varepsilon = \varepsilon_\infty$ when $\omega \gg \omega_p$; this value, $\varepsilon_\infty \cong 5-10$, is determined by transitions of electrons in occupied bands. Thus, $\varepsilon \neq 1$ within a wide frequency region, including the “metallic region,” from small ω up to a few ω_p . The dissipation rate γ for poor

metals can be quite high, on the order of a few percent, or even a few tenths of ω_p .

The manifestation of the dispersion for the frequencies corresponding to distances on the order of a few microns provides the possibility of *controlling the Casimir force by varying the parameters of the metal*. Recently, measurements of the Casimir force between a metallic sphere and a sample made with a low-conduction medium, such as silicon with different degrees of doping and vanadium dioxide VO₂, were proposed²⁰ for small separations, around 200–400 nm.

The Casimir force, including the effect of the dispersion, can be calculated for any material using its specific form of the permittivity $\varepsilon(\zeta)$, which can be found from optical data. This has been done for both good metals such as gold (see Refs. 34 and 35) and media where the metal-insulator transitions are observed (see Ref. 36). However, within this approach, the Casimir force could only be obtained *numerically*. We emphasize here that, previously, there were *no analytical* expressions to describe the Casimir force for materials within the Drude model with $\varepsilon_\infty \neq 1$: namely, Eqs. (1), (2), and (5) are *not* applicable for this case.

Here we apply the general Lifshitz theory of the *Casimir force to low-conducting compounds*, i.e., *poor metals*. We show that, for distances in the submicrometer and micrometer ranges, the Casimir force for a large variety of such systems can be described *analytically* by formulas that depend on a small number of parameters, without details of the total spectral characteristics. The inhomogeneous composite systems considered here, containing small regions of different properties, can be described within our theory. The application of these results to the region of the metal-insulator transition, where the metallic and dielectric phases coexist, produces a *drastic change of the Casimir force*. Indeed, as shown in this paper, the Casimir force can increase by a factor of 2 near this transition.

II. DERIVATION OF THE CASIMIR FORCE FOR POOR METALS

For general dispersive media, the Casimir force is determined by the integral in Eq. (4). Keeping in mind the large variety of poor-metal parameters discussed above, we now need to develop an analytical approach to estimate the integral Eq. (4) and to study the role of different parameters, such as ε_∞ or γ/ω_p , describing the system. Let us now use a two-scale model for $\varepsilon(\zeta)$ as follows:

$$\varepsilon = E(\zeta) \left[1 + \frac{\omega_p^2}{\zeta(\zeta + \gamma)} \right], \quad (6)$$

where the function $E(\zeta)$ describes the high-frequency dependence of ε . As we will show below, the detailed properties of this function are not important in the region of interest: $l \sim 1 \mu\text{m}$. The function $E(\zeta)$ is almost constant, $E(\zeta) = \varepsilon_\infty$, for all the metallic region, $\omega_p \sim \omega \ll \omega_0$, and tends to one for $\omega \gg \omega_0$. Obviously, for such a model the standard Casimir behavior in Eq. (1) is valid at large enough distances: $l > \lambda_p \sim 1 \mu\text{m}$.

To calculate the Casimir force for distances on the order of $c/\omega_p \sim 1 \mu\text{m}$ we use the general Eq. (3) rewritten as

$$F = \frac{\hbar}{2\pi^2 c^3} \left(\int_0^{\langle \omega \rangle} \zeta^3 d\zeta \Phi \left\{ \varepsilon_\infty \cdot \left[1 + \frac{\omega_p^2}{\zeta(\zeta + \gamma)} \right] \right\} + \int_{\langle \omega \rangle}^\infty \zeta^3 d\zeta \Phi[E(\zeta)] \right).$$

Here the value $\langle \omega \rangle$ is chosen in the intermediate region

$$\omega_p \ll \langle \omega \rangle \ll \omega_0.$$

Therefore, we replaced $E(\zeta)$ by ε_∞ in Eq. (6) for the first integral and omitted the Drude multiplier for the second integral.

Expanding the integration region over ζ in both integrals up to $0 \leq \zeta < \infty$, and subtracting the extra terms, we present the Casimir force in the form,

$$F = F^{(m)} + \Delta F, \quad (7)$$

with

$$F^{(m)} = \frac{\hbar}{2\pi^2 c^3} \int_0^\infty \zeta^3 d\zeta \Phi \left\{ \varepsilon_\infty \left[1 + \frac{\omega_p^2}{\zeta(\zeta + \gamma)} \right] \right\}, \quad (8)$$

$$\Delta F = \frac{\hbar}{2\pi^2 c^3} \int_0^\infty \zeta^3 d\zeta \{ \Phi[E(\zeta)] - \Phi[\varepsilon_\infty] \}. \quad (9)$$

In the frequency region, $\omega \sim c/l$, which is an important regime for $\Phi[\varepsilon(\zeta)]$, the functions $\Phi[E(\zeta)]$ and $\Phi[\varepsilon_\infty]$ in Eq. (9) almost cancel each other. Therefore, the term ΔF is relatively small. A more detailed analysis gives

$$\Delta F \cong \frac{\hbar c l_0^2}{l^6} \ll F.$$

Thus, in the region of interest, $l_0 \ll l \sim l_p$, the Casimir force is described by the first term in Eq. (7), $F = F^{(m)}$.

Now we introduce the variable $z = \zeta l/c$ and write the main contribution to the Casimir force as

$$F = \frac{\pi^2 c \hbar}{240 l^4} \cdot \Pi \equiv F_C \cdot \Pi, \quad (10)$$

where F_C is the Casimir force, Eq. (1), for ideal metals, the prefactor Π depends only on the dimensionless parameters $\tilde{l} = l/l_p$, ε_∞ , and $\alpha = \gamma/\omega_p$,

$$\Pi = \frac{120}{\pi^4} \int_0^\infty z^3 dz \int_1^\infty p^2 dp \times \left[\frac{1}{A_1^p \exp(x) - 1} + \frac{1}{A_2^p \exp(x) - 1} \right], \quad (11)$$

where A_1 and A_2 are given by Eq. (4) with

$$\varepsilon = \varepsilon_\infty \left[1 + \frac{\tilde{l}^2}{z(z + \alpha \tilde{l})} \right].$$

A. Computing the Casimir force integrals

In Sec. II A, we derive an approximation to the integral Eq. (11) for the case of poor metals with a dielectric permit-

tivity $\varepsilon(\zeta)$ in the form given by Eq. (6). This approximation is a key point of this paper and provides new analytical results for the Casimir force. We use a known approach for the evaluation of such integrals, which was successfully employed for the description of the Casimir effect at intermediate separations $l \sim l_0$ (see the monograph in Ref. 18).

Let us now change the variable z by $x=2pz$ in Eq. (11) and note that the integral

$$I = A \int_0^\infty (Ae^x - 1)^{-1} x^3 dx,$$

for constant $A \geq 1$, is monotonous in A and also a very weak function of A . Indeed, I takes the value

$$I = \frac{\pi^4}{15} \approx 6.49$$

when $A=1$, and $I=6$ for $A \rightarrow \infty$. Thus, with good accuracy, we can approximate the integrals in Eq. (11) as

$$\int_0^\infty dx \frac{x^3}{A(x,p)\exp(x) - 1} \approx \frac{\pi^4}{15A(x_0,p)} \quad (12)$$

with an appropriate value of x_0 . Here we chose the coefficient $\pi^4/15$ that is valid for the case $A \approx 1$. Due to this choice, our approximation allows a transition to the known result Eq. (1) for the limiting case of ideal metals. A numerical analysis performed using our approximation shows that all results are practically independent of the choice of the parameter x_0 in Eq. (12). For example, the difference in the values of Π in Eq. (11) obtained for $x_0=3$ (this x_0 is the position of the maximum of the function $x^3 e^{-x}$) and for $x_0=4$ (this x_0 follows from the analysis of the problem with $A=1+\varepsilon x$, $\varepsilon \ll 1$) is less than 3%.

Thus, the problem here is now reduced to calculating two one-dimensional integrals, J_1 and J_2

$$J_{1,2} = \int_1^\infty \frac{dp}{p^2} \frac{1}{A_{1,2}}, \quad \Pi = \frac{1}{2}(J_1 + J_2), \quad (13)$$

where A_1 and A_2 are given by Eq. (4) with the substitution

$$\varepsilon = \varepsilon_\infty \left[1 + \frac{4\tilde{l}^2 p^2}{x_0(x_0 + 2p\alpha\tilde{l})} \right]. \quad (14)$$

The validity of this approximation is also confirmed by the numerical calculation of the integral Eq. (11), as shown in Fig. 1. The plots in this figure show very good agreement between the results of the calculations of Π using the exact formula (11) (symbols) and the approximation Eqs. (13) and (14) with $x_0=4$ (solid lines). The function $\Pi(\tilde{l})$ found numerically is shown in Fig. 2.

A simple analysis of Eq. (13) gives us two limit cases. For small $\tilde{l} \lesssim x_0/2p_{\text{eff}}$, where p_{eff} is the characteristic value of p in the integrals in Eq. (13), where the value of α plays a minor role. Indeed, curves with different α in Fig. 2 almost coincide in the region $\tilde{l} \lesssim 0.4$. In this region, the value of Π

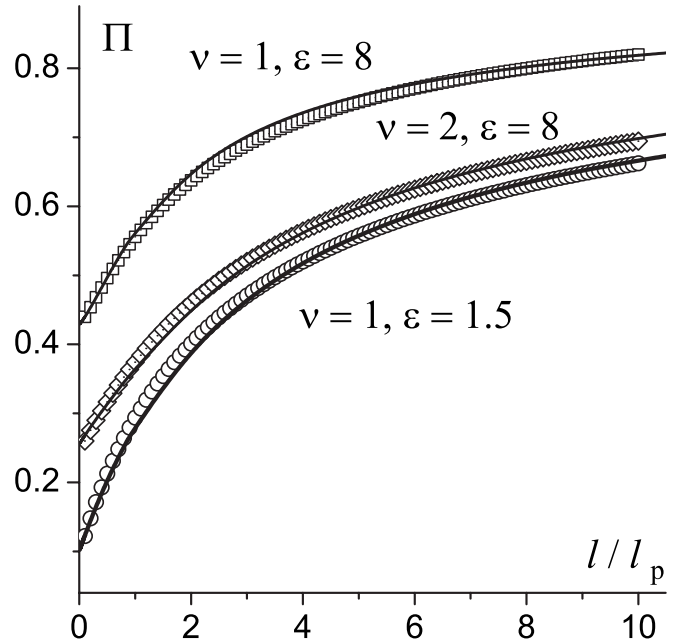


FIG. 1. The normalized Casimir force $\Pi=F/F_C$ versus l/l_p for some values of parameters (shown near curves). This plot compares the results of numerical calculations of the two-dimensional integral Eq. (11) for the prefactor Π (symbols \square , \diamond , and \circ) with the results within the approximate approach based on Eq. (13) (solid curves). This plot shows a very good agreement between both.

does not practically depend on \tilde{l} and reproduces well the Lifshitz's result (2) for dielectric media with a ζ -independent $\varepsilon=\varepsilon_\infty$ and $\gamma=0$,

$$\Pi_L \equiv \left(\frac{\varepsilon_\infty - 1}{\varepsilon_\infty + 1} \right)^\nu \cdot \varphi_\nu(\varepsilon_\infty).$$

We now emphasize that the dependence of the Casimir force, proportional to $\bar{\omega}/l^3$, see Eq. (5), is *not realized* for any $\varepsilon_\infty \neq 1$.

Otherwise, in the limit case $\tilde{l} \rightarrow \infty$, the integrals $J_1=J_2=1$, and the ideal Casimir limit, Eq. (1), is recovered. In contrast to the case of small values of \tilde{l} , the dependence of Π on l for large, but finite, values of \tilde{l} shows an interesting and unexpected behavior: the approach to saturation is *quite slow*, especially for large values of

$$\alpha = \frac{\gamma}{\omega_p}.$$

In other words, it is hard to reach the metallic limit value of $\Pi=1$ when $\alpha > 0.1$, for the most interesting region $\tilde{l} \lesssim 10$.

To understand this behavior, let us now investigate in more details the factor Π for not so small values of \tilde{l} . As mentioned above, it is a sum of two contributions from the electromagnetic fields of different polarizations. It is convenient to separately examine the first and second integrals. Numerical calculations show that the behavior of these two integrals, J_1 and J_2 , is essentially different for the same values of parameters, as shown in Fig. 3.

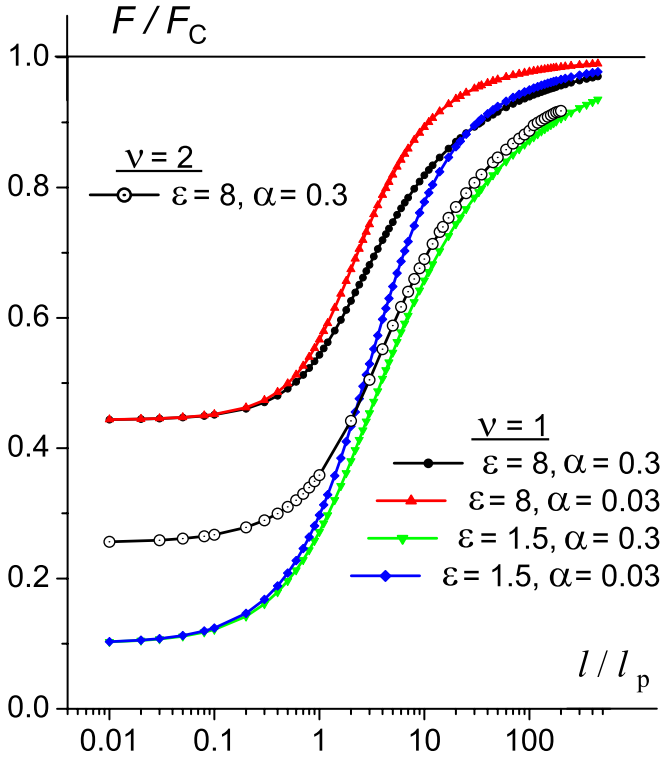


FIG. 2. (Color online) The normalized Casimir force $\Pi = F/F_C$ versus the parameter $\tilde{l} = l/l_p$, for $\nu=1,2$, using the typical value $\varepsilon_\infty=8$, as well as the smaller $\varepsilon_\infty=1.5$, and different values of the dissipation parameter $\alpha = \gamma/\omega_p$. The horizontal line on top gives the asymptotic value, $F/F_C = \Pi = 1$, for an ideal metal.

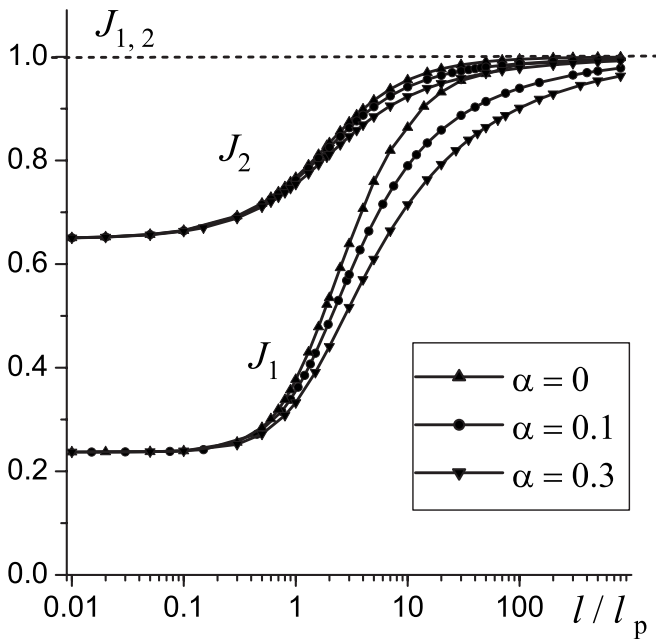


FIG. 3. Integrals J_1 and J_2 , defined by Eq. (13), describing the Casimir force versus l/l_p for $\varepsilon_\infty=8$ and different values of the dissipation parameter $\alpha = \gamma/\omega_p$. The symbols indicated inside the square depict the results of numerical calculations.

The two interesting features (i.e., the slow approach to saturation and the essential dependence of Π on $\alpha = \gamma/\omega_p$) are mostly associated with the first integral, J_1 , which describes the contribution of the fluctuations with the electric field parallel to the surfaces of plane-parallel samples. This integral J_1 can be calculated analytically. For $\alpha=0$, it can be written as

$$J_1 = 1 - \frac{2}{b} \cdot \ln \left(\frac{\sqrt{a^2 + b^2} + b}{a} \right) + \frac{4}{b\sqrt{a^2 - 1}} \cdot \arctan \left(\frac{\sqrt{a^2 - 1}}{a + 1} \cdot \frac{\sqrt{a^2 + b^2} + b - a}{\sqrt{a^2 + b^2} + b + a} \right), \quad (15)$$

where we introduce the notation

$$a^2 = 1 + \varepsilon_\infty \frac{4\tilde{l}^2}{x_0^2}, \quad b^2 = \varepsilon_\infty - 1.$$

For nonzero dissipation rate, $\alpha \neq 0$, the analytical formula for J_1 is very long and inconvenient for real estimates.

The complex behavior of the function $\Pi(\tilde{l})$ and the role of the dissipation constant α can be clarified by means of the asymptotics of J_1 for large separations. For any finite value of α and extremely large \tilde{l} (when $\tilde{l} \gg 1, 1/\alpha$), J_1 versus \tilde{l} has a very slow inverse-square-root dependence,

$$J_1 \approx 1 - 4 \sqrt{\frac{\alpha x_0}{2\tilde{l}\varepsilon_\infty}} \quad \tilde{l} \gg 1, 1/\alpha. \quad (16)$$

For very small $\alpha \ll 1$, the intermediate region $1/\alpha \gg \tilde{l} \gg 1$ can also be considered. For this region, the behavior of J_1 is sharper,

$$J_1 \approx 1 - \frac{x_0}{\sqrt{\varepsilon_\infty}} \cdot \frac{1}{\tilde{l}}, \quad 1/\alpha \gg \tilde{l} \gg 1. \quad (17)$$

Using a simple fitting procedure, we have found a formula which approximates well the function $J_1(\tilde{l})$,

$$J_{1,\text{appr}} = \frac{\sqrt{(3 + \varepsilon_\infty)(3 + 5\alpha\tilde{l}) + 3\varepsilon_\infty\tilde{l}^2} - 2\sqrt{3 + 5\alpha\tilde{l}}}{\sqrt{(3 + \varepsilon_\infty)(3 + 5\alpha\tilde{l}) + 3\varepsilon_\infty\tilde{l}^2} + 2\sqrt{3 + 5\alpha\tilde{l}}}, \quad (18)$$

as shown in Fig. 4. This simple expression can be useful for a description of the experimental data.

An analytical expression for J_2 in terms of elementary functions cannot be written. Fortunately, the integral J_2 exhibits a simpler behavior than J_1 and for its description we can use a simple approximation. First note the quite weak dependence of the shape of the function $J_2(\tilde{l})$ on the value of α , as shown in Fig. 5. For the regime of interest here, $\varepsilon_\infty \gg 1$, the difference between the values of J_2 for $\alpha=0.3$ and $\alpha=0$ is maximum near the range $\tilde{l} \sim (10-15)$ and does not exceed 3%. Indeed, all the curves with $0 \leq \alpha < 0.3$ merge together and for describing J_2 within an accuracy of 1.5%,

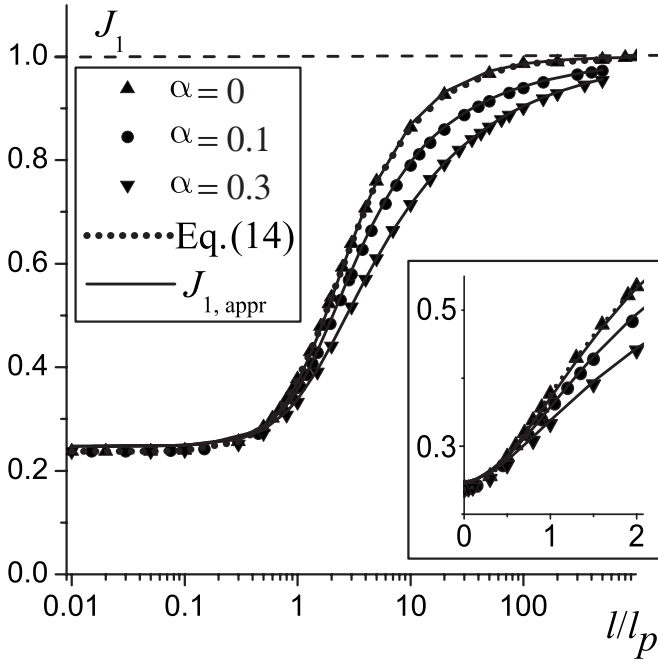


FIG. 4. The integral J_1 versus l/l_p for $\epsilon_\infty=8$ and different values of the dissipation parameter $\alpha=\gamma/\omega_p$ (indicated by the symbols inside the square). The symbols depict the results of numerical calculations. The detailed behavior of J_1 for small \tilde{l} is present in the inset. The dotted line describes the analytical result Eq. (15) for $\alpha=0$, solid lines are drawn in accordance with the fitting formula (18).

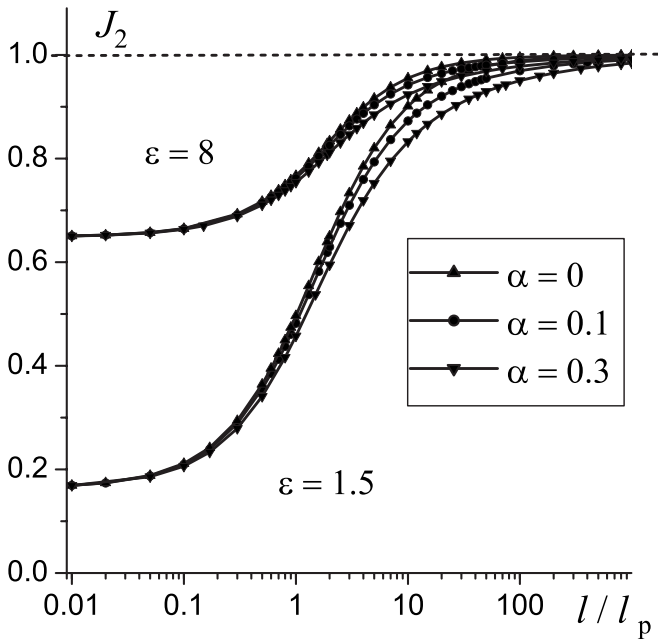


FIG. 5. The integral J_2 versus l/l_p , calculated numerically for $\epsilon_\infty=8$ and $\epsilon_\infty=1.5$ and different values of α (indicated by the symbols inside the square). The shapes of the curves $J_2(l/l_p)$ depend very weakly on α .

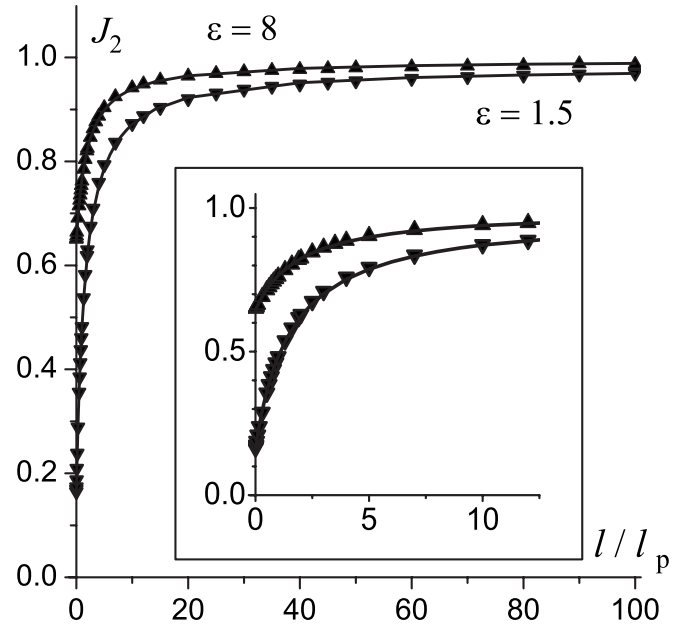


FIG. 6. The integral J_2 versus l/l_p , calculated numerically for $\alpha=0.1$ and very different values of the dielectric permittivity, $\epsilon_\infty=8$ (\blacktriangle) and $\epsilon_\infty=1.5$ (\blacktriangledown). The curves describe the approximating function Eq. (19). Note the very good agreement between numerical data and approximating functions. The inset shows the magnified curves for small values of l/l_p .

the function $J_2(\tilde{l})$ found for $\alpha=0.1$ can be used. Even for small $\epsilon_\infty=1.5$, the inaccuracy of this approximation is less than 5%.

Numerical data are well fitted by the very simple formula

$$J_{2,\text{fit}} = \frac{J_{2,L} + \eta \tilde{l}}{1 + \eta \tilde{l}}, \quad (19)$$

where $\eta \approx (0.5-0.6)$, $J_{2,L}$ determines the value of J_2 for small $\tilde{l} \ll 1$, as shown in Fig. 6. The quantity $J_{2,L}$ describes the contribution of J_2 to the Lifshitz's result (2) for dielectric media with $\epsilon=\epsilon_\infty$ and $\alpha=0$.

Thus, we can present a simple description of the second integral J_2 : it is practically independent on the dissipation parameter α and the dependence on ϵ_∞ is governed only by the Lifshitz contribution $J_{2,L}$. The asymptotic behavior of J_2 at large distances $\tilde{l} \gg 1$ is of the form $1 - (1 - J_{2,L}) / \eta \tilde{l}$, which is much weaker than the inverse-square-root dependence, Eq. (16), for J_1 . For large $\epsilon_\infty \gg 1$, when $(1 - J_{2,L}) \propto 1/\epsilon_\infty \ll 1$, the dependence $J_2(\tilde{l})$ is especially weak, even compared with that for J_1 in the intermediate region, Eq. (17).

B. Change of the Casimir force near the metal-insulator transition

The analytical formulas derived above give a good description of the behavior of the Casimir force when the metal-insulator transition occurs. Usually, the metal-insulator transition is associated with an abrupt change, by a few orders of magnitude, of the conductivity at a transition tem-

perature $T=T_c$. Let us start with a rough picture, assuming that a metallic phase has a finite value of the plasma frequency whereas for the dielectric phase the plasma frequency is zero. Using the results obtained above, one can expect a drastic change of the Casimir force between two plane-parallel samples caused by the change of the parameter l_p , very near the metal-insulator transition.

We stress that the change of the force is not connected with changing the *physical* distance l , but with changing the *dimensionless* quantity $\tilde{l}=l/l_p$, caused by the *change of the plasma wavelength* $\lambda_p=2\pi l_p=2\pi c/\omega_p$. Thus, one can expect a *jumplike behavior of the Casimir force when changing the temperature across T_c* . Within the transition region, the force changes from the “metallic” value $F^>$, typical for finite values of \tilde{l} , to the very different value $F^<$, for an insulator when $\tilde{l}\ll 1$.

The important quantity here is the change of the Casimir force, $\Delta F=(F^>-F^<)$. To estimate $F^<$, we can use the Lifshitz formula (2) valid in the limit $l\ll l_p$, which corresponds to the dielectric phase. The value of $F^>$ in the metallic phase corresponds to large but finite values of l/l_p . To estimate $F^>$, note that the dependence of Π on l at $10\gtrsim l/l_p\gtrsim 2.5$ is mainly provided by the integral J_1 , whereas J_2 can be replaced by one. Thus, the concrete value of the coefficient η in Eq. (19) is not important. Combining all these data together, and restoring the initial parameters of the media, ω_p and γ , we arrive at the simple estimate,

$$\Delta F = \frac{\pi^2 c \hbar}{240 l^4} \cdot \left[1 - \left(\frac{\varepsilon_\infty - 1}{\varepsilon_\infty + 1} \right) \varphi_1(\varepsilon_\infty) - \frac{2}{\omega_p} \sqrt{\frac{c \gamma x_0}{2 \varepsilon_\infty l}} \right], \quad (20)$$

where the function $\varphi_1(\varepsilon)$ describes the Lifshitz’s result for the interaction of a dielectric sample and an ideal metal. When the value of γ is small enough, as for manganites, for the distance l such that $l\ll c/\gamma$, Eq. (17) is valid, and the formula for ΔF reads

$$\Delta F = \frac{\pi^2 c \hbar}{240 l^4} \cdot \left[1 - \left(\frac{\varepsilon_\infty - 1}{\varepsilon_\infty + 1} \right) \varphi_1(\varepsilon_\infty) - \frac{c x_0}{2 \omega_p l \sqrt{\varepsilon_\infty}} \right]. \quad (21)$$

Note that our results differ significantly from the theoretical estimates given in Ref. 20. In particular, the value of ΔF in Ref. 20 is proportional to the temperature T . The linear dependence ΔF on T can be expected for large enough separations $l\gg c\hbar/kT$, that is, larger than a few microns and cannot appear for small separations.

It is worth noting that the relative change of the force

$$\Delta F = \frac{F^> - F^<}{F^>}$$

is larger for long distances l , when the value $F^>$ of the force for media in the conducting state is larger than the limit value $F^<$ describing the case of small ω_p and small l/l_p . This feature is determined by the quite slow change of the function $\Pi(\tilde{l})$ at not so small values of ε_∞ , as shown in Fig. 2.

III. COMPOSITE MEDIA AND THE INTERMEDIATE REGION FOR METAL-INSULATOR TRANSITION

The very abrupt (by a few orders of magnitude) change of the conductivity at the metal-insulator transition occurs for the dc case only. At finite frequencies, the behavior of the complex permittivity of compounds near metal-insulator transition is more complicated and the jumplike behavior, typical for the static conductivity, does not arise for $\varepsilon=\varepsilon(i\xi)$. Within the finite transition region, the presence of a nonuniform state with coexisting metallic and insulator phases is well established for all systems showing a metal-insulator transition. Obviously, this effect is of great interest for studying the Casimir force. The effective-medium approach suggests that the metallic and insulating regions coexist as interpenetrating clusters, providing a percolation picture³⁷ of the metal-insulator transition at $T=T_c$. When the transition is of first order, the phase-separated regions are mesoscopic, in the 100 nm range, and quasistatic objects (giant clusters) have approximately equal electron densities.

To describe the Casimir force for such a nonuniform state, we have used the effective-medium approximation,³⁷ developed for different composite media. This approach was used for studying the reduction in the Casimir force for porous dielectrics.³⁸ This approximation has been used for explaining the optical properties of VO_2 near the metal-insulator transition.³⁹ In this model, the effective value of $\varepsilon=\varepsilon_{\text{eff}}(\xi)$ is determined by the concentration $f(0\leq f\leq 1)$ of the metal phase following the equation,

$$f \cdot \frac{\varepsilon_m - \varepsilon_{\text{eff}}}{\varepsilon_m + (d-1)\varepsilon_{\text{eff}}} + (1-f) \cdot \frac{\varepsilon_i - \varepsilon_{\text{eff}}}{\varepsilon_i + (d-1)\varepsilon_{\text{eff}}} = 0, \quad (22)$$

where ε_m and ε_i are the frequency-dependent permittivities for the metallic and insulating phases, respectively. Also, $d=2$ and $d=3$ for the thin film (thickness smaller than the grain size) and bulk sample, respectively. In the intermediate region, the effective permittivity $\varepsilon_{\text{eff}}(i\xi)$ as a function of the phase concentration f can be written as follows:

$$2 \frac{\varepsilon_{\text{eff}}(i\xi)}{\varepsilon_\infty} = (2f-1) \frac{\omega_p^2}{\xi(\xi+\gamma)} + \sqrt{4 + \frac{4\omega_p^2}{\xi(\xi+\gamma)} + \left[\frac{(2f-1)\omega_p^2}{\xi(\xi+\gamma)} \right]^2} \quad \text{for } d=2, \quad (23)$$

and

$$4 \frac{\varepsilon_{\text{eff}}(i\xi)}{\varepsilon_\infty} = 1 + (3f-1) \frac{\omega_p^2}{\xi(\xi+\gamma)} + \sqrt{9 + \frac{6(1+f)\omega_p^2}{\xi(\xi+\gamma)} + \left[\frac{(3f-1)\omega_p^2}{\xi(\xi+\gamma)} \right]^2} \quad \text{for } d=3. \quad (24)$$

These equations predict an infinite value of $\varepsilon_{\text{eff}}(i\xi)$ when $\xi\rightarrow 0$ (that corresponds to a metallic conductivity) when $f_c\leq f\leq 1$ only, where $f_c=1/d$ is a percolation threshold, see

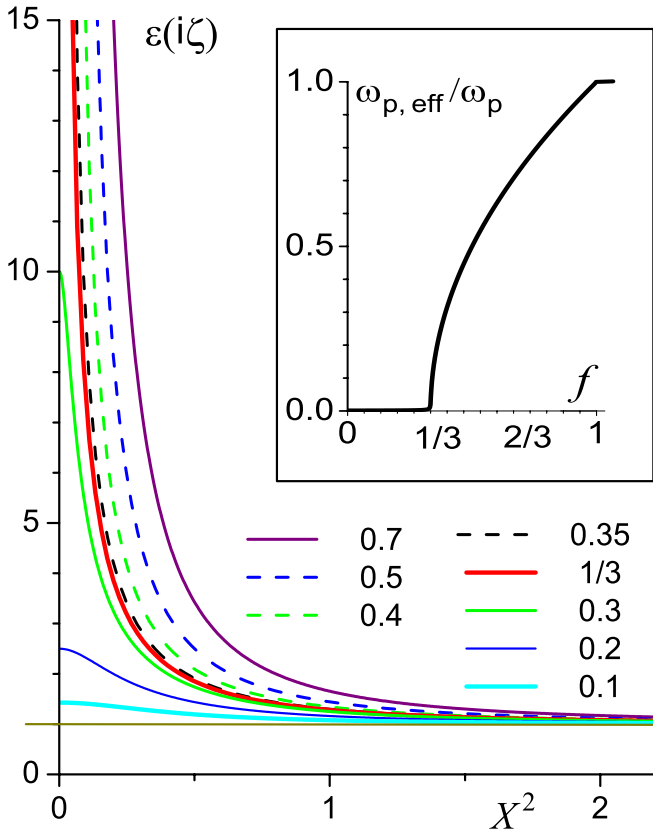


FIG. 7. (Color online) The effective permittivity $\varepsilon_{\text{eff}}(i\zeta)$ (in units of ε_∞), for $d=3$ and different concentrations f of the metal phase, as a function of the dimensionless variable $X^2 = \zeta(\zeta + \gamma)/\omega_p^2$. Inset: effective plasma frequency $\omega_{p,\text{eff}}$ (in units of ω_p) versus f in the coexistence region.

Fig. 7. Otherwise, a dielectric behavior is present with a finite value of $\varepsilon_{\text{eff}}(i\zeta)$ when $\zeta \rightarrow 0$,

$$\varepsilon_{\text{eff}}(\zeta = 0) = \frac{\varepsilon_\infty}{1 - fd} > \varepsilon_\infty, \quad \text{for } f < \frac{1}{d},$$

as shown in Fig. 7. In the metallic region (above the percolation threshold, for $f > f_c$), the behavior of $\varepsilon_{\text{eff}}(i\zeta)$ at small ζ is determined by the effective plasma frequency $\omega_{p,\text{eff}}$,

$$\varepsilon_{\text{eff}} \rightarrow \varepsilon_\infty \frac{\omega_{p,\text{eff}}^2}{\zeta(\zeta + \gamma)} \quad \text{when } \zeta \rightarrow 0.$$

The value of $\omega_{p,\text{eff}}^2$ increases linearly with f from zero, at $f = f_c$, until ω_p^2 , at $f = 1$. Thus, a square-root behavior of the effective plasma frequency $\omega_{p,\text{eff}}$ over $(f - f_c)$ is present in the metallic region, see inset in Fig. 7.

It is useful to note here that a linear temperature dependence of ω_p^2 was observed⁴⁰ in $\text{La}_{0.7}\text{Sr}_{0.3}\text{MnO}_3$ for $T < T_c$. Thus, we can describe the Casimir force in the intermediate region as a series of curves with their shape only depending on l/l_p , as shown in Fig. 8.

IV. PREDICTIONS FOR SPECIFIC MATERIALS

Using the results obtained in the previous sections, here we estimate numbers for different materials showing the

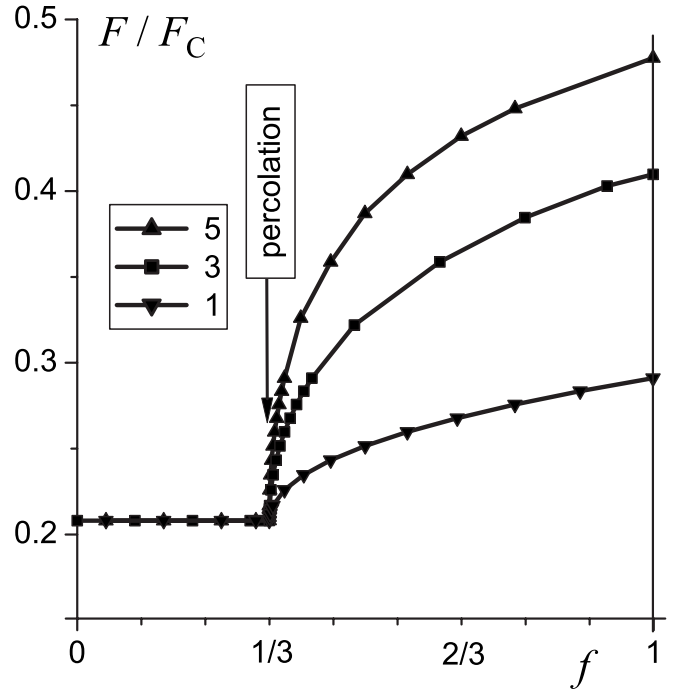


FIG. 8. Casimir force for the interaction between two equivalent poor metals ($\nu=2$) (with $\varepsilon_\infty=8$ and $\alpha=0.3$) versus the concentration f of the metallic phase in the coexistence region. The force is normalized by values of the force F_C for ideal metals in the same geometry and for different values of $l/l_p=1$ (\blacktriangledown), 3(\blacksquare), and 5(\blacktriangle), where l_p is determined by the plasma frequency in the pure metallic phase.

metal-insulator transition. To study the Casimir force in the vicinity of the metal-insulator transition, we choose two typical compounds: vanadium dioxide VO_2 and the manganites exhibiting colossal magnetoresistance. For these two materials, the general Drude behavior of permittivity with typical values of λ_p on the order of $1 \mu\text{m}$ and with relatively large values of ε , $\varepsilon_\infty \sim 5-10$, is observed in the infrared region of interest.

A. Vanadium dioxide VO_2

Vanadium dioxide, VO_2 , shows a jump in the static conductivity (a metal-insulator transition) a little bit above room temperature, at $T = T_c \approx 68^\circ\text{C}$. The pure metallic phase of VO_2 is realized at $T > 88^\circ\text{C}$, and pure insulator phase³¹ (more exactly, semiconducting phase with a gap on the order of 1 eV) at $T < 60^\circ\text{C}$. For vanadium dioxide, the phase separated state has been observed³⁹ within a finite-temperature range, between 60°C and 88°C , by measuring the optical properties of VO_2 . Recently, such state was directly observed⁴¹ via scanning tunneling spectroscopy. For all temperatures where the metallic conductivity is present, the generalized Drude behavior is observed up to infrared frequencies, with a relatively large value of $\varepsilon_\infty \cong 9$ and $\lambda_p = 2\pi c/\omega_p \cong 1 \mu\text{m}$. The phonon contribution to the value of ε , typical for the infrared region, is screened by free carriers, and the value of $\varepsilon_\infty \cong 9$ is kept until the high-frequency region, with wavelength $\lambda \leq 0.1 \mu\text{m}$, where the value of (ε

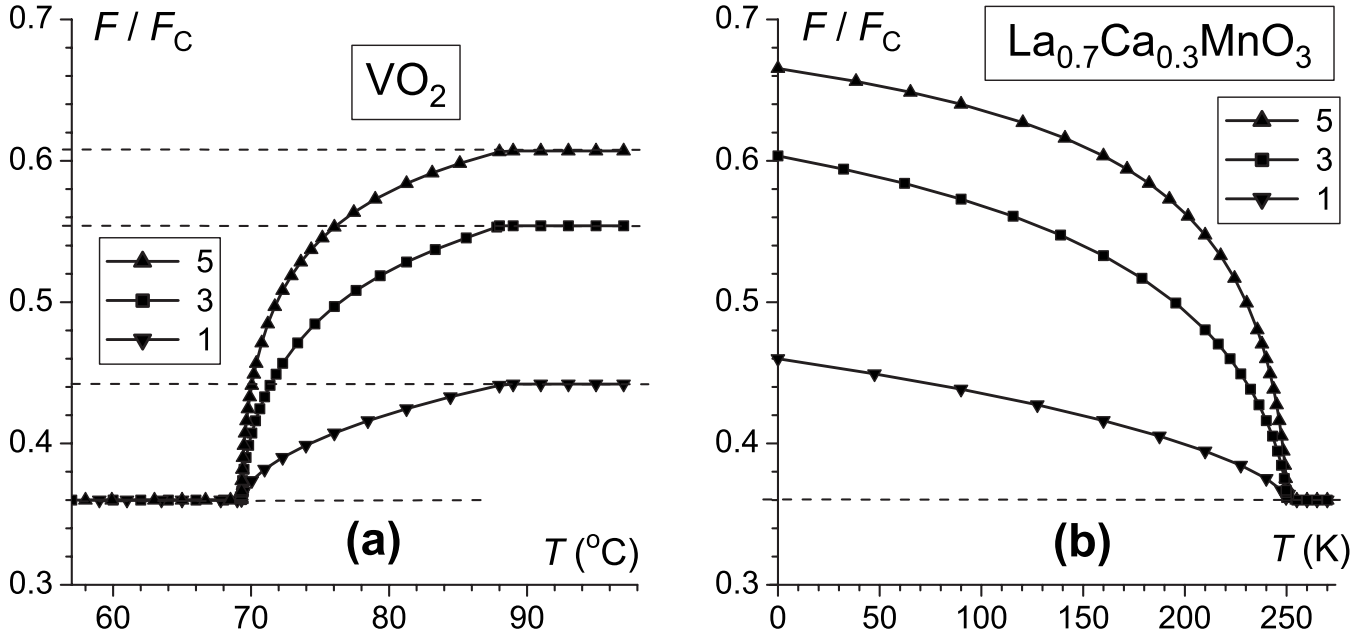


FIG. 9. Predicted dependence of the Casimir force on temperature for the interaction between a poor metal and an ideal metal, calculated for (a) VO₂ and for (b) La_{0.7}Ca_{0.3}MnO₃. The force is normalized by its value F_C for an ideal metal for different values of $l/l_p=1$ (\blacktriangledown), 3 (\blacksquare), and 5 (\blacktriangle), where l_p is determined by the plasma frequency in the pure metallic phase. The horizontal dashed lines indicate the limit values of the force for the pure insulating phase and (for VO₂ only) its metallic phase. The corresponding values of F_C are described by Eq. (1); for $\lambda_p \approx 1.2 \mu\text{m}$ these are $F_C=0.9$, 1.15×10^{-2} , and $1.5 \times 10^{-3} \text{ dyn/cm}^2$ for $l/l_p=1, 3$, and 5 , respectively. Note that the Casimir force can increase by about a factor of 2.

–1) vanishes. The value of the dissipation rate γ for this compound is large enough, $\gamma/\omega_p \sim 0.3$ for VO₂, and the data for large α should be considered.

For VO₂, the Casimir force increases when increasing the temperature through the transition region, from 60 °C until 88 °C, see Fig. 9(a). Our analysis shows that this dependence is strongly affected by the presence of dissipation. The value of α is quite high and the calculated change of the Casimir force is essentially smaller than for the naive estimate [i.e., the difference between the values F_C for an ideal metal and F_L for a dielectric, see Eqs. (1) and (2)]. For this reason, the relative change of the Casimir force is maximal for large enough distances, e.g., $l \approx 5l_p \approx 1 \mu\text{m}$. This result is in agreement with Ref. 36 where the dependence of the Casimir force for VO₂ on the distance l was numerically calculated for temperatures below and above the metal-insulator transition. Here we present the temperature dependence of the Casimir force in the *whole* transition region both using analytical and numerical approaches.

B. Manganites

Manganites (with antiferromagnetic insulators LaMnO₃ or NdMnO₃ as parent compounds after substitution of La by divalent ion) show a metal-insulator transition at the dopant concentration $x \sim 0.3$, with a ferromagnetic metallic phase in the low-temperature range.³³ These systems are very popular now in the context of colossal magnetoresistance based on the possibility of the metal-insulator transition induced by an external magnetic field, that is, caused by the ferromagnetic ordering of the metallic phase. On the other hand, the stan-

dard temperature-induced metal-insulator transition is possible for such materials as well. For example, the typical compound La_{0.7}Ca_{0.3}MnO₃ demonstrates a metal-insulator transition at $T=T_c=250 \text{ K}$. The phase-separation state is present for all temperatures below the transition point and a linear temperature dependence of $\omega_{p,\text{eff}}^2$ has been observed³⁷ in this region. Note that this metal-insulator transition is accompanied by ferromagnetic ordering. In principle, it could produce an extra force of magnetic origin near the transition (antiferromagnetic ordering present for some metal-insulator transition does not produce any source of long-ranged interactions). However, for large enough plane-parallel samples, the magnetic-flux lines are closed inside the magnetic sample, and should not produce any serious parasitic effects. For these compounds, ω_p is small and the corresponding $\lambda_p \sim 1 \mu\text{m}$. The main specific feature important for us here is the low value of the dissipation rate: typical values of γ/ω_p are $\sim 0.02-0.05$, and the low- γ behavior of the curves shown in Figs. 2 and 3 are adequate.

For La_{0.7}Ca_{0.3}MnO₃, the metallic phase corresponds to the low-temperature range, and the value of the force increases when decreasing the temperature, which leads to an opposite temperature behavior of the Casimir force, compared to VO₂. The value of α for this compound is relatively low and the dependence of the Casimir force on T is sharper than for the previous example. One more specific feature is the presence of phase separation in the whole region of the metallic phase existence. Thus, one can expect an essential dependence of the Casimir force for all temperatures below the transition temperature, see Fig. 9(b).

V. DISCUSSION

The Casimir force depends on the materials used and we have studied some of these material-dependent aspects. The Casimir force F_C for a mechanical system containing compounds with a metal-insulator transition shows a *drastic change* in the transition region. The relative change ΔF_C of the force, when crossing the transition region, can be quite large, on the order of the force itself for a distance ~ 1 micron. Thus the Casimir force would become twice as large in this regime. The relative change ΔF_C of the Casimir force is even larger for large distances, where the absolute value of the force is small. However, for short distances, e.g., $l=l_p \sim 0.2 \mu\text{m}$, the relative change of the Casimir would be much smaller, on the order of 20% (in contrast to the 100% increase for $l \sim 1$ micron). The dependence of the force on temperature is sharp near the percolation threshold, where the static metallic conductivity appears.

When measuring such tiny forces, the exclusion of any parasitic effects, such as electrostatic forces, is essential. To avoid electrostatic forces, the usual highly conducting samples are short circuited.¹³ This method might appear to be ineffective for the metal-insulator transition compounds near the insulating region. However, such compounds are more semiconducting than insulating in this region and the conductivity is nonzero at room temperatures. Thus, we believe that the same technique could be used. To increase the conductivity in the semiconducting region, the usual doping by donor or acceptor impurities could be used. Finally, we note that the metal-insulator transition is sometimes accompanied by structural phase transitions, which could lead to some lattice distortions. Thus, care should be taken to choose materials and operating conditions that avoid these additional difficulties.

For measurement of the Casimir force for samples made with usual metals, small separations are preferable. The cre-

ation of experimental setups with very small (submicrometer) distances between samples is a serious challenge for experimentalists. As follows from our analysis, distances l comparable with the plasma wavelength λ_p are preferable for the experimental observation of the effects, we predict around the region of the metal-insulator transition. For the compounds discussed above, this means distances on the order of $1 \mu\text{m}$. In the planned experiments²⁰ for measuring the Casimir force using vanadium oxide samples, the separations are $(0.2-0.4) \mu\text{m}$, which equals $(0.15-0.3)\lambda_p$. These values are much smaller than the optimal values noted above. For separations l on the order of $0.1\lambda_p$, that is $0.6l_p$, the Casimir force should follow low- l asymptotics for any temperature (in both the metallic and the insulating phases). The temperature dependence of the Casimir force should be weak and the manifestation of the metal-insulator transition should be minor for such an experimental setup.

ACKNOWLEDGMENTS

We gratefully acknowledge partial support from the National Security Agency (NSA), Laboratory of Physical Sciences (LPS), Army Research Office (ARO), National Science Foundation (NSF) under Grant No. EIA-0130383, JSPS-RFBR under Grant No. 06-02-91200. E.G.G. and B.A.I. acknowledge partial support from the joint Grant No. 219-09 from the Russian Foundation for Basic Research and Ukrainian Academy of Science, and from Ukrainian Academy of Science via Grant No. VC 38/V 139-18. S.S. acknowledges support from the grant Ministry of Science, Culture and Sport of Japan via the Grant-in-Aid for Young Scientists No. 18740224, the EPSRC via Grants No. EP/D072581/1 and No. EP/F005482/1, and ESF network-program ‘‘Arrays of Quantum Dots and Josephson Junctions.’’

*bivanov@i.com.ua

¹H. B. G. Casimir, Proc. K. Ned. Akad. Wet. **51**, 793 (1948).

²P. W. Milonni, *The Quantum Vacuum: An Introduction to Quantum Electrodynamics* (Academic, San Diego, 1994).

³K. A. Milton, *The Casimir Effect: Physical Manifestations of Zero-point Energy* (World Scientific, Singapore, 2001).

⁴M. Kardar and R. Golestanian, Rev. Mod. Phys. **71**, 1233 (1999).

⁵M. Bordag, U. Mohideen, and V. M. Mostepanenko, Phys. Rep. **353**, 1 (2001).

⁶F. Capasso, J. N. Munday, D. Iannuzzi, and H. B. Chan, IEEE J. Sel. Top. Quantum Electron. **13**, 400 (2007).

⁷S. K. Lamoreaux, Rep. Prog. Phys. **68**, 201 (2005); Phys. Today **60**(2), 40 (2007).

⁸C. Cattuto, R. Brito, U. M. Marconi, F. Nori, and R. Soto, Phys. Rev. Lett. **96**, 178001 (2006).

⁹J. M. Obrecht, R. J. Wild, M. Antezza, L. P. Pitaevskii, S. Strin-gari, and E. A. Cornell, Phys. Rev. Lett. **98**, 063201 (2007).

¹⁰S. K. Lamoreaux, Phys. Rev. Lett. **78**, 5 (1997).

¹¹U. Mohideen and A. Roy, Phys. Rev. Lett. **81**, 4549 (1998);

F. Chen, G. L. Klimchitskaya, U. Mohideen, and V. M. Mostepanenko, Phys. Rev. A **69**, 022117 (2004).

¹²G. Bressi, G. Carugno, R. Onofrio, and G. Ruoso, Phys. Rev. Lett. **88**, 041804 (2002).

¹³V. Petrov, M. Petrov, V. Bryksin, J. Petter, and T. Tschudi, Opt. Lett. **31**, 3167 (2006).

¹⁴C. Genet, A. Lambrecht, and S. Reynaud, Phys. Rev. A **62**, 012110 (2000).

¹⁵D. Iannuzzi, M. Lisanti, J. N. Munday, and F. Capasso, Solid State Commun. **135**, 618 (2005); J. N. Munday, D. Iannuzzi, Yu. Barash, and F. Capasso, Phys. Rev. A **71**, 042102 (2005); J. N. Munday, D. Iannuzzi, and F. Capasso, New J. Phys. **8**, 244 (2006); D. Iannuzzi, M. Lisanti, J. N. Munday, and F. Capasso, J. Phys. A **39**, 6445 (2006); J. N. Munday and F. Capasso, Phys. Rev. A **75**, 060102(R) (2007); J. N. Munday, F. Capasso, and V. A. Parsegian, Nature (London) **457**, 170 (2009).

¹⁶H. B. Chan, V. A. Aksyuk, R. N. Kleiman, D. J. Bishop, and F. Capasso, Science **291**, 1941 (2001); Phys. Rev. Lett. **87**, 211801 (2001).

¹⁷E. M. Lifshitz, Sov. Phys. JETP **2**, 73 (1956).

- ¹⁸E. M. Lifshitz and L. P. Pitaevskii, *Statistical Physics, Part 2* (Pergamon, Oxford, 1980).
- ¹⁹I. E. Dzyaloshinskii, E. M. Lifshitz, and L. P. Pitaevskii, *Sov. Phys. Usp.* **4**, 153 (1961).
- ²⁰R. Castillo-Garza, C.-C. Chang, D. Jimenez, G. L. Klimchitskaya, V. M. Mostepanenko, and U. Mohideen, *Phys. Rev. A* **75**, 062114 (2007).
- ²¹L. P. Pitaevskii, *Phys. Rev. Lett.* **101**, 163202 (2008).
- ²²D. A. R. Dalvit and S. K. Lamoreaux, *Phys. Rev. Lett.* **101**, 163203 (2008).
- ²³V. B. Svetovoy, *Phys. Rev. Lett.* **101**, 163603 (2008).
- ²⁴J. Blocki, J. Randrup, W. J. Swiatecki, and C. F. Tsang, *Ann. Phys. (N.Y.)* **105**, 427 (1977).
- ²⁵D. E. Krause, R. S. Decca, D. López, and E. Fischbach, *Phys. Rev. Lett.* **98**, 050403 (2007).
- ²⁶G. Bimonte, E. Calloni, G. Esposito, and L. Rosa, *Nucl. Phys. B* **726**, 441 (2005); G. Bimonte, E. Calloni, G. Esposito, and L. Rosa, *J. Phys. A* **39**, 6161 (2006).
- ²⁷G. Palasantzas, P. J. van Zwol, and J. Th. M. De Hosson, *Appl. Phys. Lett.* **93**, 121912 (2008).
- ²⁸V. A. Yampol'skii, S. Savel'ev, Z. A. Mayselis, S. S. Apostolov, and F. Nori, *Phys. Rev. Lett.* **101**, 096803 (2008); V. A. Yampol'skii, S. Savel'ev, Z. A. Mayselis, S. S. Apostolov, and F. Nori, *ibid.* **103**, 039901(E) (2009).
- ²⁹V. A. Yampol'skii, S. Savel'ev, Z. A. Mayselis, S. S. Apostolov, and F. Nori, arXiv:0905.1462 (unpublished).
- ³⁰F. S. S. Rosa, D. A. R. Dalvit, and P. W. Milonni, *Phys. Rev. Lett.* **100**, 183602 (2008).
- ³¹N. F. Mott, *Metal-Insulator Transitions*, 2nd ed. (Taylor & Francis, London, 1990); M. Imada, A. Fujimori, and Y. Tokura, *Rev. Mod. Phys.* **70**, 1039 (1998).
- ³²*High Temperature Superconductivity*, edited by K. S. Bedell, D. Coffey, D. E. Meltzer, D. Pines, and J. R. Schrieffer (Addison-Wesley, Reading, MA, 1990).
- ³³*Physics of Manganites*, edited by T. A. Kaplan and S. D. Mahanti (Kluwer Academic/Plenum, New York, 1999).
- ³⁴I. Pirozhenko, A. Lambrecht, and V. B. Svetovoy, *New J. Phys.* **8**, 238 (2006).
- ³⁵V. B. Svetovoy, P. J. van Zwol, G. Palasantzas, and J. Th. M. De Hosson, *Phys. Rev. B* **77**, 035439 (2008).
- ³⁶I. Pirozhenko and A. Lambrecht, *Phys. Rev. A* **77**, 013811 (2008).
- ³⁷T. W. Noh, P. H. Song, and A. J. Sievers, *Phys. Rev. B* **44**, 5459 (1991).
- ³⁸R. Esquivel-Sirvent, *J. Appl. Phys.* **102**, 034307 (2007).
- ³⁹H. S. Choi, J. S. Ahn, J. H. Jung, T. W. Noh, and D. H. Kim, *Phys. Rev. B* **54**, 4621 (1996).
- ⁴⁰K. H. Kim, J. H. Jung, and T. W. Noh, *Phys. Rev. Lett.* **81**, 1517 (1998).
- ⁴¹Y. J. Chang, C. H. Koo, J. S. Yang, Y. S. Kim, D. H. Kim, J. S. Lee, T. W. Noh, H. T. Kim, and B. G. Chae, *Thin Solid Films* **486**, 46 (2005).